Influence of northwest Indian Ocean sea surface temperature and El Niño–Southern Oscillation on the winter precipitation in Iran

Ahmad Reza Ghasemi

ABSTRACT

This paper studies the impact of northwest Indian Ocean (NIO) sea surface temperature (SST) anomalies between the regions 0–29°N and 45–80°E and El Niño–Southern Oscillation (ENSO) on the winter precipitation in Iran. The data include monthly precipitation from 45 weather stations in Iran, monthly NIO SST with a 2° horizontal resolution and Southern Oscillation Index (SOI) for a 40-year period (1975–2014). This study utilizes canonical correlation analysis and partial correlation to investigate the simultaneous relationship between SST, SOI, and winter precipitation variability. A running correlation method is also used to test the stationarity of these relationships. Analyses of the results reveal that both NIO SST and ENSO index are significantly correlated with the winter precipitation in Iran but with opposite sign. Moreover, a clear variability exists in the correlations revealing a distinct non-stationarity in the relationship over time. The results of partial correlation analysis suggest that the ENSO index has a stronger effect on the winter precipitation in Iran than NIO SST.

Key words | canonical correlation analysis, ENSO, Indian Ocean SST, Iran, winter precipitation

Ahmad Reza Ghasemi
Water Engineering Department, Agricultural Faculty,
Shahrekord University,
Shahrekord,
Iran
E-mail: *ghasemiar@yahoo.com*; *ar-ghasemi@sku.ac.ir*

INTRODUCTION

Due to water resources limitation in Iran, studying precipitation variability is of particular importance. Iran is mainly an arid and semi-arid region, so the investigation of precipitation variability and its moisture sources can be an effective and useful means to enhance water management capabilities. The regional precipitation changes can be due to the climate patterns such as El Niño–Southern Oscillation (ENSO) and Ocean's sea surface temperature (SST) changes. The oceans cover about 70% of the global surface and have a significant influence on Earth's climate and its variations (Herr & Galland 2009). Because of their large heat-storage capacity, they continuously exchange moisture with the atmosphere by means of the water cycle. Ocean SST plays an important role in the air–sea interaction (El-Geziry 2013), as well as shaping the global climate (Houghton *et al.* 1996). It has also been proposed that SST variations can directly impact the distribution of precipitation over land; however, the effect of SST on precipitation varies regionally (Ma & Xie 2013; Yinyin *et al.* 2014).

Iran is close to the northwestern part of the Indian Ocean; therefore, its climate variability may be controlled, at least partly, by the Indian Ocean. Variations of SST in the Indian Ocean can play a primary role in modulating rainfall in neighboring continental regions (Risbey *et al.* 2009). Over the last few decades, a large number of studies has examined the association between the Indian Ocean SST and precipitation in various countries using seasonal and annual time intervals (e.g. Lu & Lu 2015). In recent years, there has been increasing interest in the investigation

doi: 10.2166/wcc.2019.274

of Indian Ocean SST–ENSO interactions and possible relationships with regional precipitation variability.

Our review of the literature indicates that a limited number of studies has examined the impact of Indian Ocean sea surface temperatures on precipitation in Iran. For instance, Nazemosadat (1996) showed that positive anomalies of autumn precipitation in Iran generally happen at the same time as positive anomalies of the Arabian Sea SST. Nazemosadat & Ghasemi (2006) also showed that the Indian Ocean SST (12°N to 18°N and 60°E to 66°E) is positively correlated with winter (January to March) precipitation in southern Iran. Overall, these studies concluded that winter precipitation in Iran has a negative relationship with the SST in some parts of the Indian Ocean.

Generally, it can be concluded that considering both ENSO and Indian Ocean SST may improve results when studying precipitation and its prediction in Iran. Therefore, the present paper attempts to study the winter precipitation variability in Iran during combined ENSO and northwest Indian Ocean's (NIO) SST.

MATERIALS AND METHODS

Iran lies between latitudes 24° and 40°N and longitudes 44° and 64°E and shares borders with the Gulf of Oman and the Persian Gulf in the south and the Caspian Sea in the north (Figure 2). In general, Iran has a mostly arid climate (based on the Koppen climate classification) with an average annual precipitation of about 250 mm. The distribution of the annual and also winter precipitation reveals a strong gradient with higher values corresponding to the western parts of the Caspian Sea coast and lower values obtained for the southeast of Iran (Ghasemi & Khalili 2008). In comparison to the annual precipitation, the percentages of the winter precipitation in Iran vary from 70% to 20%. On average, about 44% of the annual precipitation in Iran occurs in the winter considered as the main portion of annual precipitation at most stations. Figure 1 shows the monthly precipitation in Iran. Winter and autumn are the wettest seasons and summer is the driest season in Iran.

Analyses are performed on two main datasets, including the monthly SST over the NIO and the observed precipitation corresponding to 45 weather stations throughout Iran for the period 1975 to 2014 (Figure 2).

The observed precipitations are obtained from Iran Meteorological Organization and the SSTs data set from the NCEP/NCAR reanalysis archive website with a grid resolution of 2° in latitude and longitude. For the purpose of the present study, 187 grid points within the NIO region (0–29°N and 45–80°E) were selected (Figure 2). Meteorological winter is defined as being December–February.

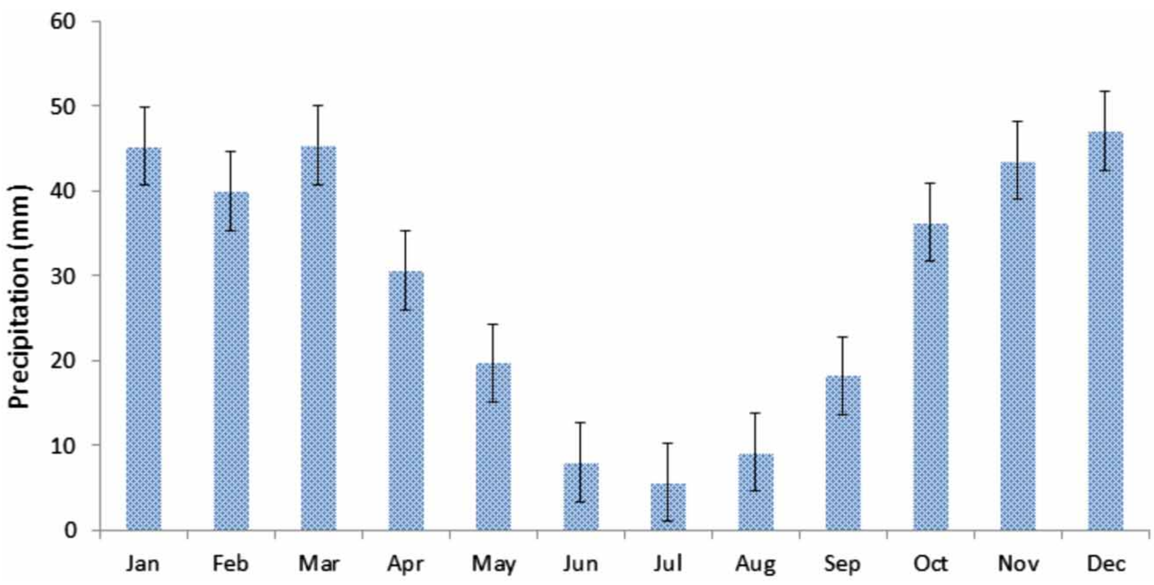

Figure 1 | Monthly precipitation in Iran.

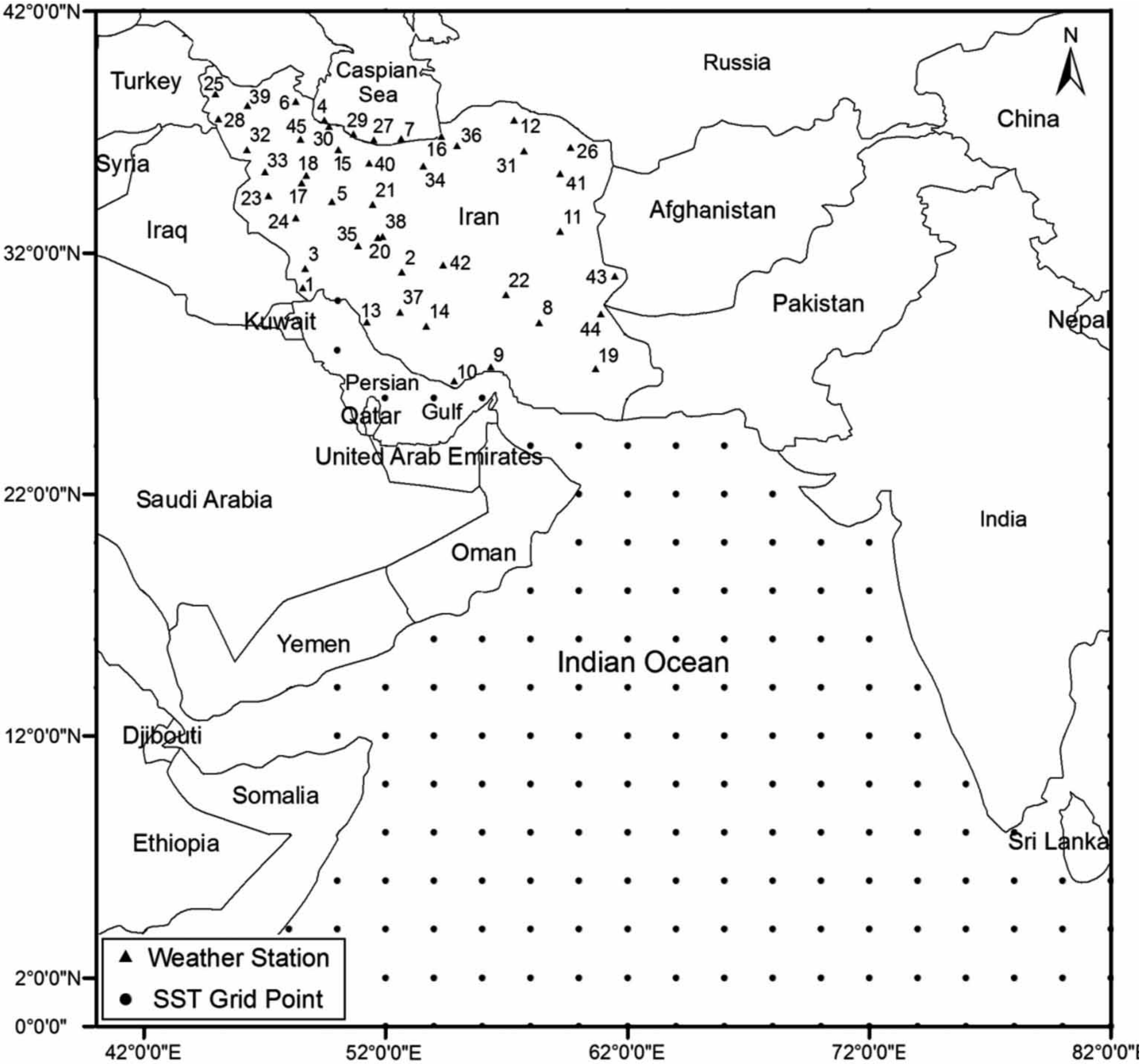

1	Abadan	9	BandarAbbas	17	Hamedan	25	Khoy	33	Sanandaj	41	Torbat
2	Abadeh	10	BandarLengeh	18	Nojeh	26	Mashhad	34	Semnan	42	Yazd
3	Ahwaz	11	Birjand	19	Iranshahr	27	Noushahr	35	Shahrekord	43	Zabol
4	Anzali	12	Bojnord	20	Isfahan	28	Oromieh	36	Shahroud	44	Zahedan
5	Arak	13	Boushehr	21	Kashan	29	Ramsar	37	Shiraz	45	Zanjan
6	Ardabil	14	Fassa	22	Kerman	30	Rasht	38	Shragh Isf.		
7	Babolsar	15	Ghazvin	23	Kermanshah	31	Sabzevar	39	Tabriz		
8	Bam	16	Gorgan	24	Khoramabad	32	Saghez	40	Tehran		

Figure 2 | Map of the study area showing the weather stations in Iran and grid points locations for the northwest Indian Ocean SST.

At the first step, a principal component analysis (PCA) is applied. The purpose of PCA is to reduce a dataset containing a large number of variables (here, 45 precipitation series in Iran and 187 SST series in NIO) to a dataset containing fewer new variables called principal component time series (PCs) (Wilks 1995). The scree plot is used to visually assess components or factors explaining most of the variability in the data. The number of preserved modes of SST is $p=4$ (87% of the variation is explained by the first four PCs), and for precipitation, it is $q=3$ (54% of the variability in the original data is explained by the first three PCs).

At the second step, these PCs are used as input to the canonical correlation analysis (CCA). The CCA method is performed to measure the simultaneous relation between winter precipitation in Iran and NIO's SST variability. In constructing the CCA model, pre-filtering and orthogonalization are done separately both on predictor (the X variable, here SST) and predictand (the Y variable, here precipitation) using PCA, which have been recommended and used by many researchers (e.g., Berri & Bertossa 2004; Barnston & Tippett 2017).

The CCA is a statistical procedure that firstly identifies a linear combination called the first canonical variate from each multivariate datasets separately (precipitation's PCs and SST's PCs). The analysis continues by finding a second linear combination (second canonical variate) from each set, and so on (Nicholls 1987). The method produces I and J linear combinations for dependent variables (precipitation's PCs), v_p, and the observed predictor (SST's PCs), w_p, respectively. Then by projecting the original data (PCs) onto these linear combinations, two new sets of variables are constructed (canonical variate):

$$v_{\mathrm{p}} = \sum_{i=1}^{I} a_{pi}\mathrm{PC_i} \quad p = 1, \ldots, \min(I, J)$$
$$w_{\mathrm{p}} = \sum_{j=1}^{J} b_{pj}\mathrm{PC}_j \quad p = 1, \ldots, \min(I, J) \tag{1}$$

where a_{pi} and b_{pj} are the vectors of weight (Wilks 1995).

In this study, CCA transforms each one of predictor and predictand variables (SST and precipitation's PCs, respectively) into three new data series (min (3, 4)) or three modes.

The canonical maps show the correlations at specific locations between the canonical variate and the time series of the SST and precipitation anomalies fields (Diaz *et al.* 1998). In this study, the first two modes of the canonical maps are considered (e.g., the first canonical map of SST shows the correlation between the first new time series of SST and original SST anomalies fields). In order to estimate the significance of the values in the canonical maps, a standard Student's *t*-test is used.

By considering significant correlation coefficients areas on the canonical maps of mode 1 and mode 2, a few oceanic and continental regions are selected (see the following). A running correlation method based on 15-year overlapping windows is also used to investigate the relationship between SST in the oceanic regions, ENSO index (Southern Oscillation index, SOI), and precipitation in the continental regions time series. The running correlation is a useful technique to identify the instability of the relationships between two variables over time, which is widely used in climate research (e.g. Slonosky *et al.* 2001; Dong & Dai 2015).

In addition, a partial correlation technique is applied to show the relationship between two variables while controlling the influences of another variable. This method is used to reveal correlations masked by the other variables (Pillai & Mohankumar 2010). For example, the impact of SST on precipitation (Pre) is defined as follows after removing the impact of ENSO on both of them:

$$r_{\mathrm{SST,Pre-ENSO}} = \frac{r_{\mathrm{SST,Pre}} - r_{\mathrm{SST,ENSO}} \times r_{\mathrm{ENSO,Pre}}}{\sqrt{(1 - r^2_{\mathrm{SST,ENSO}})} \times \sqrt{(1 - r^2_{\mathrm{ENSO,Pre}})}} \tag{2}$$

where r is Pearson's correlation coefficient.

RESULTS AND DISCUSSION

The CCA between NIO SST and winter precipitation in Iran

The first canonical maps (CCA mode 1) of the winter for SST and precipitation are shown in Figure 3(a) and 3(b), respectively. The correlation coefficients larger than 0.31 are statistically significant at the 95% level (shaded areas). The same sign (positive or negative correlations) in the canonical maps, showing the relationship between oceanic

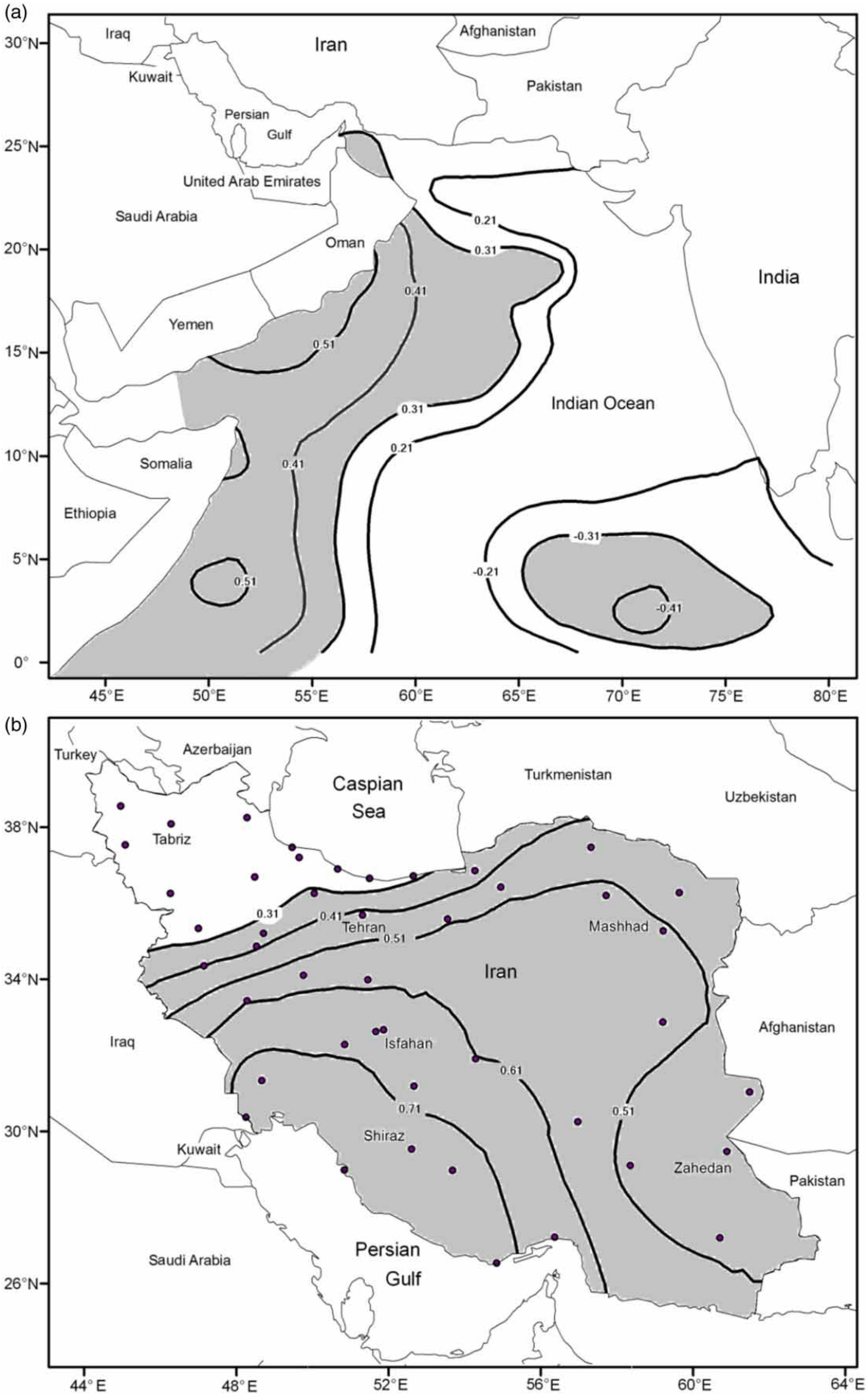

Figure 3 | (a) First canonical map (CCA mode 1) of December–February SST anomalies of the northwest Indian Ocean, (b) first canonical map of December–February for Iran winter precipitation. The shaded areas represent the regions where the correlation coefficients are significant at the 95% level.

regions and winter precipitation is of warm–wet/cold–dry type and for opposite sign is of warm–dry/cold–wet type (Berri & Bertossa 2004).

As clearly seen in Figure 3(a), there is a dipole in the studied oceanic region, a large significant region over the western half, and another significant region with the opposite sign over the southeastern parts. The latter pole is almost coincident with the Arabian Sea Mini Warm Pool. The warm pole was reported by Shenoi *et al.* (1999) and is an effective factor on the Indian summer monsoon (Nagamani *et al.* 2016).

The relationship between the western pole (Figure 3(a)) and Iran winter precipitation (shaded area in Figure 3(b)) is of warm–wet/cold–dry type because the canonical maps show patterns with the same sign. The relationship for the southeastern pole (Figure 3(a)) and Iran winter precipitation is of warm–dry/cold–wet type because the canonical maps show patterns with the opposite sign.

In comparison to CCA mode 1, in the second canonical precipitation map (CCA mode 2), only a small significant region has remained over the north and northwestern parts and other significant regions have disappeared (Figure 4(b)). On the other hand, the SST pattern exhibits a large positive significant region over south and east and a small negative significant region over Persian Gulf (Figure 4(a)). These regions have a warm–wet/cold–dry and warm–dry/cold–wet type of relationship with the winter precipitation variability over the northern parts of Iran, respectively (Figure 4(b)).

Influence of NIO SST on the winter precipitation in Iran

As shown in Figures 3(a) and 4(a), there are a few significant regions in NIO (the shaded areas), so it is difficult to find the relative importance of different oceanic regions on the winter precipitation variability in Iran. For this purpose, as mentioned in the 'Materials and Methods' section, four oceanic regions over NIO (shown by boxes in Figure 5(a), named as: W – mode 1, S–E – mode 1, PG – mode 2, and S&E – mode 2) and five continental regions over Iran (shown by boxes in Figure 5(b) named as A – mode 1, SW – mode 1, SE – mode 1, N&NE – mode 2, and NE – mode 2) were selected.

The median running correlation (MRC) coefficients between the selected oceanic regions and winter precipitation sub-regions in Iran measured by 15-year running correlations are shown in Table 1. The MCR is the median of the running correlation coefficients series (Cordery & Opoku-Ankomah 1994).

As shown in Table 1, the SST anomaly in the western parts of the studied oceanic region (W – mode 1) is significantly correlated with the most selected regions over Iran, whereas other oceanic regions have a lesser and insignificant influence, except for the South and East NIO box (S&E – mode 2). The fairly high correlation between W – mode 1 and A – mode 1 (winter precipitation over Iran except for the northwest) suggests the possible influence of the NIO SST on winter precipitation in Iran. Nazemosadat (1996) also pointed out that this area is a moisture source region for Iran through the upper-air circulation. This region also has anomalous water vapor influx into Iran by means of Sudanese low pressure. The Sudan low is a dynamic low pressure in winter that brings humidity through Arabian Peninsula to Iran (Rasuly *et al.* 2012).

The correlations have been studied in greater detail by running correlations, based on 15-year overlapping periods between each of the oceanic regions and Iran regions series to assess stability. This method offers an opportunity to test the stationarity of the relationships over time (Slonosky *et al.* 2001). Almost all of the running correlation coefficient time series between the oceanic regions and Iran winter precipitation series show some variation.

Running correlation between the winter precipitation in Iran (A – mode 1) and NIO SST (W – mode 1) is displayed in Figure 6. As it can be clearly observed, the relationships have variations in the strength over time. There is a fairly low correlation in the mid-1970s (1975–1990) that gradually rises to a peak of 0.75 in the 1980s (meaning that over 56% of the variance in Iran winter precipitation is explained by concurrent W – mode 1 SST variations) and then drops suddenly in the late 1990s.

The cycles of low and high correlations show non-stationarity in the relationship between winter NIO SST and Iran winter precipitation over the studied period. A similar non-stationarity can be seen in the relationship between the other oceanic regions and winter precipitation in Iran sub-regions (not shown).

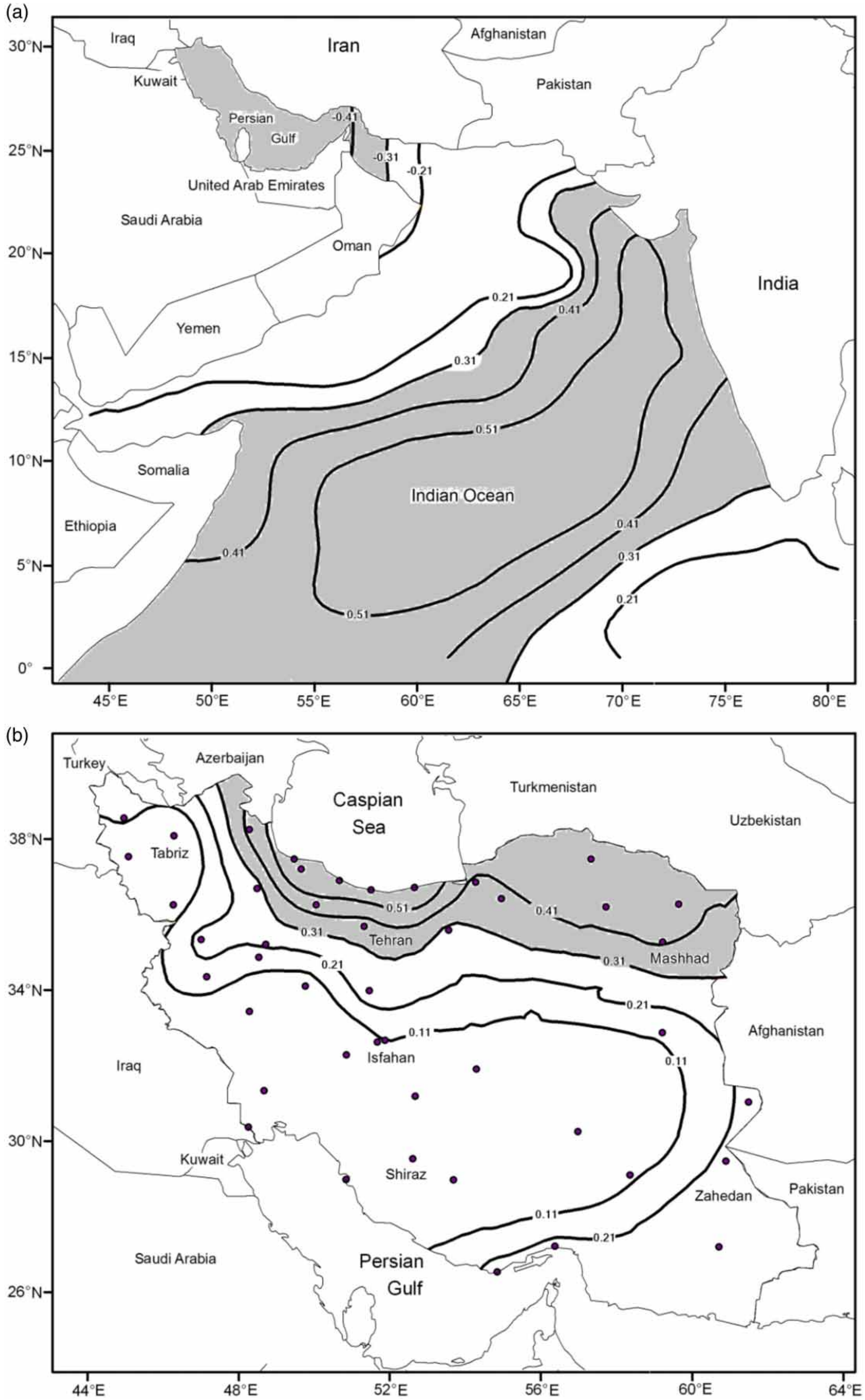

Figure 4 | The same as Figure 3, but for the second canonical map (CCA mode 2).

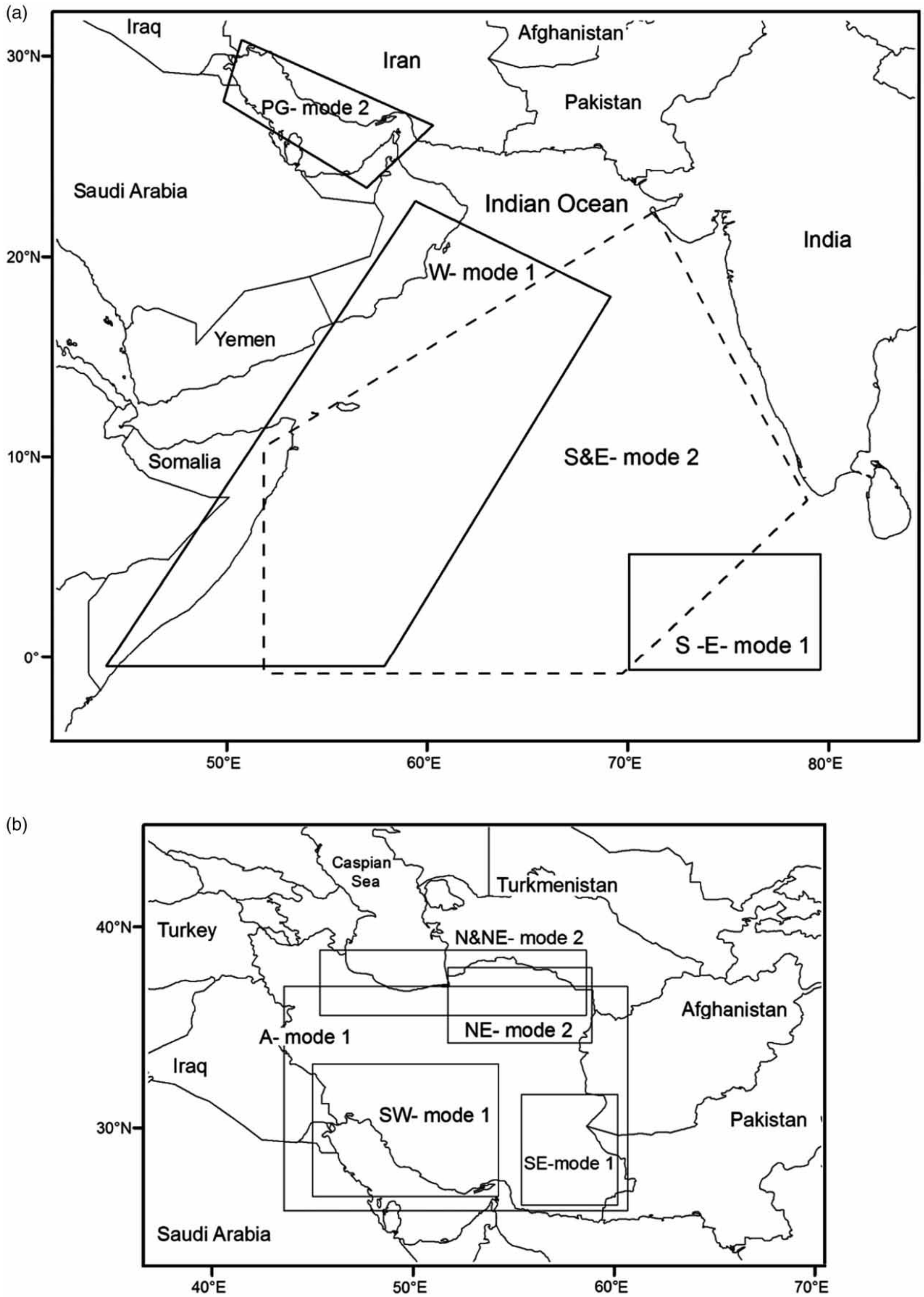

Figure 5 | (a) Oceanic regions for spatial SST averages and (b) Iran regions for spatial precipitation averages (shown by boxes).

Table 1 | The median running correlation (MRC) coefficients between the spatial SST average of every oceanic region and the spatial precipitation average of every Iran box during December–February. Numbers in bold are statistically significant at the 95% confidence level

Sub-region	W-mode 1	S-E-mode 1	PG-mode 2	S&E-mode 2
A-mode 1	**0.67**	−0.17	0.13	0.5
SW-mode 1	**0.61**	−0.23	0.17	0.4
SE-mode 1	0.42	−0.11	0.33	0.32
N&NE-mode 2	**0.61**	0.05	−0.13	**0.6**
NE-mode 2	0.54	0.06	0.02	0.49

The running correlation with 25-year overlapping windows shows a significant positive relationship between NIO SST and Iran winter precipitation (Figure 6). However, the correlations have become weak but statistically significant in recent years. Ghasemi & Khalili (2008) also found a positive relationship between wet and dry conditions in Iran and north Indian Ocean SST. By decreasing the length of the time period (15-year overlapping windows), the correlations are noticeably weakened and nonsignificant in recent years (Figure 6). As the relationship between winter NIO SST and Iran winter precipitation is positive, it is more possible that the dry and wet years in Iran occur in cold and warm Indian Ocean SST, respectively. From 2008 to 2014, Iran has been experiencing drought conditions (normalized precipitation less than −0.5), but in this period, only in 1 year (2011), the drought conditions in Iran are coincident with cold winter NIO SST (normalized SST less than −0.5) and in 2 years (2010 and 2013), the drought conditions have inverse relationship with NIO SST, leading to weak correlation between these two variables over this period.

Additionally, to estimate the uncertainty involved in the application of short-term database (1975–2014), the correlation coefficients for this period were compared with 99% confidence interval of the correlation during the period of 1958–2014. There are 20 stations with longer precipitation database (1958–2014) in A – mode 1 box (Figure 5(b)). The 99% confidence interval of the correlation between the area-average precipitation and winter NIO SST during this period (1958–2014) is calculated and illustrated in Figure 6. As shown in this figure, all running correlation coefficients are in the range of 99% confidence interval.

Precipitation relationship with SOI

Many researchers demonstrated that the ENSO is a coupled ocean–atmosphere which accounts for a significant portion of climate variability around the globe. The winter precipitation over sub-regions of Iran shows a negative correlation with the simultaneous ENSO index. The coefficients are significant at the 95% level for winter average

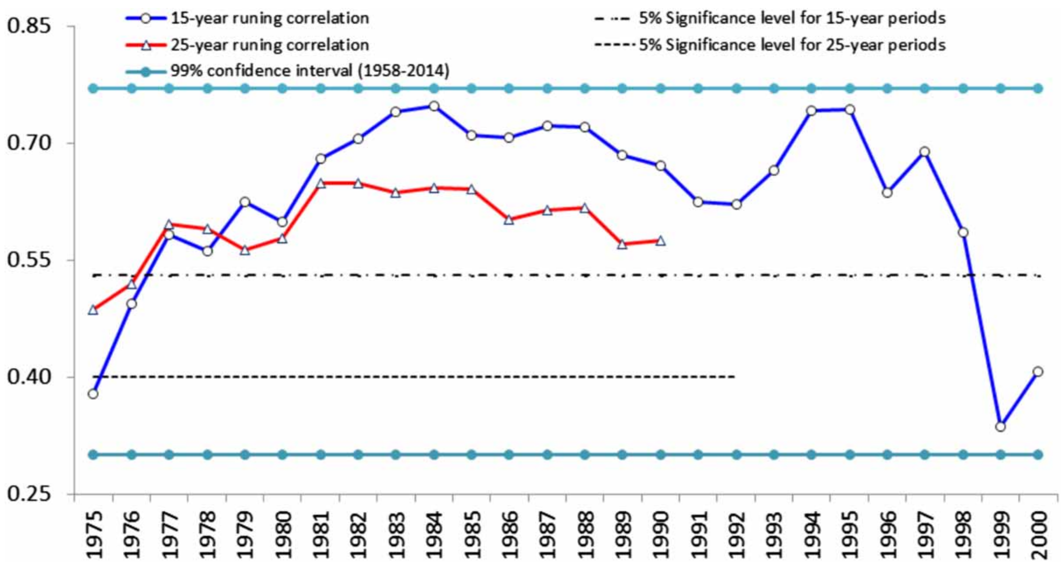

Figure 6 | Running correlations over 15- and 25-year windows between winter SST over W-mode 1 and concurrent winter precipitation in A-mode 1. The starting year of each period is shown by the horizontal axis.

Table 2 | The median running correlation (MRC) coefficients between the spatial precipitation average of every Iran box and SOI. Numbers in bold are statistically significant at the 95% confidence level

Sub-region	MSC-15
A-mode 1	**−0.56**
SW-mode 1	−0.44
SE-mode 1	−0.2
N&NE-mode 2	**−0.63**
NE-mode 2	**−0.65**

precipitation over Iran (A – mode 1) and northern sub-regions (N&NE – mode 2 and NE – mode 2) (Table 2), suggesting that El Niño conditions are associated with wetter conditions and La Niña with drier conditions. The percentage of wet and dry conditions associated with El Niño and La Niña events in sub-regions of Iran are represented in Table 3. As clearly seen, the percentage of wet conditions in Iran during El Niño events varies from 40% to 63% and during La Niña from 8% to 20%. These values are 8% to 25% and 46% to 60% for dry conditions.

Since the A – mode sub-region encompasses a large portion of Iran, it is used for a more detailed analysis. As shown in Figure 7, the running correlation between ENSO index and Iran winter precipitation (A – mode 1) is very low at the first 15-year period (1975–1989) but gradually is increased thereafter. The statistically significant ENSO-precipitation correlation coefficients are found for the time periods since 1984. The period 1998–2012 shows the strongest correlation at a value of −0.79, which can be considered as a period of relative maximum influence of the ENSO on Iran winter precipitation variability.

The robustness of the conclusions is shown by the increased length of window width (25-year) (Figure 7). The ENSO-precipitation relations have been stronger in recent years. However, the short span of the studied period can be a constraint in the data analysis.

These results may be explained by the increased number of the winter El Niño and La Niña events during the recent decades. There are only 6 ENSO events (4 El Niño and 2 La Niña) in the first half of the studied period (1975–1994),

Table 3 | The percentage of wet and dry conditions in sub-regions of Iran associated with El Niño and La Niña events

Sub-region	A-mode 1		SW-mode 1		SE-mode 1		N&NE-mode 2		NE-mode 2	
	El Niño	La Niña	El Niño	La Niña	El Niño	La Niña	El Niño	La Niña	El Niño	La Niña
Wet	50	10	50	10	40	20	63	13	63	13
Dry	11	56	8	58	10	60	25	50	18	46

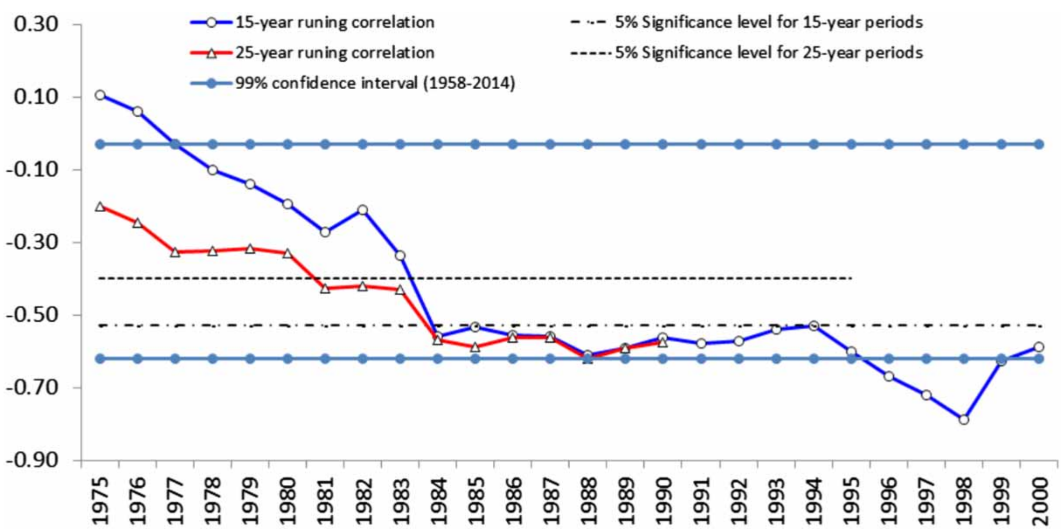

Figure 7 | As for Figure 6 but between winter SOI and concurrent winter precipitation in A – mode 1.

while in the second half (1995–2014), there are a total of 11 ENSO events, 8 (3) of them are La Niña (El Niño). All winter La Niña years during the second half are associated with below-normal winter precipitations in A – mode 1 sub-region and two of three El Niño events are associated with above-normal precipitations (not shown).

SST relationship with SOI

Many previous studies have reported that the Indian Ocean variability is strongly related to ENSO variability (Manjunatha *et al.* 2015). Our finding also revealed a significant negative correlation (−0.42) between the SOI index and the winter SST anomalies in both western parts of the NIO (W – mode 1) and S&E – mode 2 over a 15-year overlapping window. Other studied oceanic regions show no significant correlation coefficient. Yuan *et al.* (2008) showed that SST in the northwestern Indian Ocean is closely correlated with the ENSO. In addition, Roxy *et al.* (2014) reported a high relationship between the western Indian Ocean warming and ENSO index during summer.

The correlations between NIO SST and SOI have been studied in greater detail by expanding the overall correlations into running correlations (Figure 8). The variation in the strength of the correlations (15 and 25-year) shows non-stationarities of the relationship between the SOI and SST. The ENSO index and SST in W – mode 1 are very highly correlated in the late 1990s, with a peak of 0.83 (meaning that about 69% of the variations in SST are explained by the variations of SOI) in 1998–2012 window. As a result, it is concluded that, similar to the ENSO-precipitation relation, the linkage between W – mode 1 SST and ENSO index has been stronger in recent years (since 1996 and 1988 for 15- and 25-year sliding windows, respectively). As illustrated in Figure 8, however, the significant running correlation coefficients for 15-year window are not in the range of 99% confidence interval in recent years; all correlation coefficients for 25-year window are in the range of 99% confidence interval.

For example, all correlation coefficients in 15-year overlapping windows are significant and show a sharp decreasing trend (stronger correlation coefficients) since 1993. It is worth noting that there is a substantial increase in the number of ENSO events since 1993. There are 16 ENSO events since 1993 (6 El Niño and 10 La Niña) and only 8 events before it; 5 out of 6 El Niño events are coincident with positive STT anomaly in NIO and 8 out of 10 La Niña events are coincident with negative NIO SST anomaly (not shown). This could well explain the stronger relationship between ENSO and NIO SST in the recent decades.

Partial correlation

The above results clearly suggest that SST over the western Indian Ocean has a significant association with the ENSO index, as well as winter precipitation in Iran. There is an

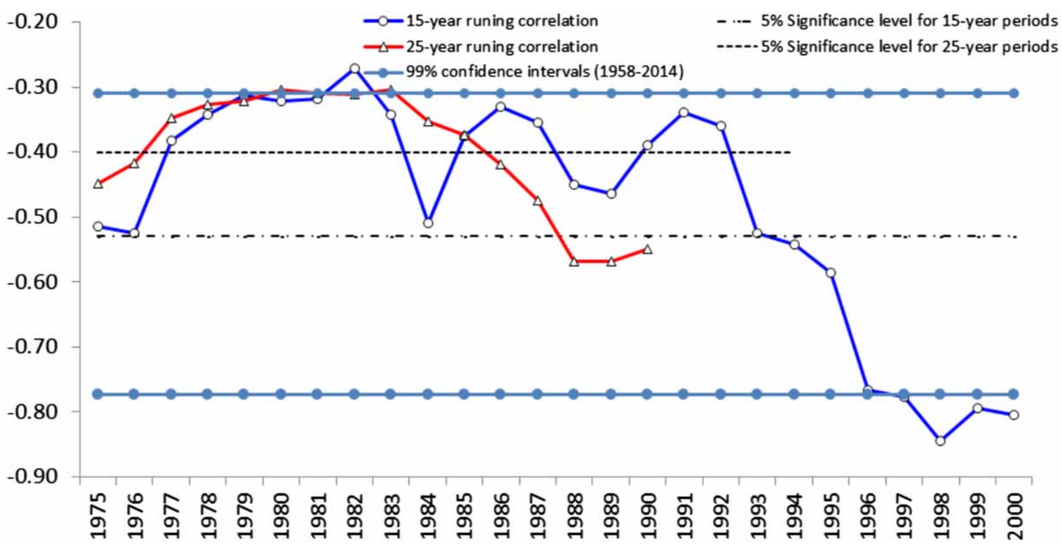

Figure 8 | As for Figure 6 but between winter SST over northwest Indian Ocean and concurrent SOI.

important debate about whether the Indian Ocean SST is entirely controlled by ENSO or its variability is independent of ENSO (Krishnamurthy & Kirtman 2003).

Partial correlation analysis is carried out to find the effect of SST on precipitation after excluding the effect of SOI on both precipitation and SST. If precipitation is directly forced by the fluctuations of the SST, then the correlation should still exist in the partial correlation results. In other words, it was investigated if the NIO SST is an independent index for explaining winter precipitation variability in Iran, or it reflects the effect of ENSO.

The partial correlation of precipitation (A – mode 1) and SST (W – mode 1) suppressing ENSO and that of precipitation and ENSO restraining SST are given in Table 4. MRC coefficients are also seen in this table. From Table 4, it is clear that when the effect of ENSO is suppressed, the correlation becomes very weak and insignificant ($r = 0.15$). These results would suggest that both W – mode 1 SST and winter precipitation are influenced by ENSO index. These results are supported by the significant running correlation between ENSO and precipitation ($r = -0.56$) and SST ($r = -0.43$). Similarly, the correlation between precipitation and ENSO is also decreased ($r = -0.21$) when the effect of SST is removed.

On the basis of the above, it can be concluded that in the absence of ENSO (the removal of ENSO effect from 'NIO SST-Iran winter precipitation' relationship), the SST relationship with the precipitation becomes weaker than the absence of SST (the removal of NIO SST effect from 'ENSO-Iran winter precipitation' relationship). This suggests that although ENSO has a stronger effect on Iran winter precipitation than NIO SST, both phenomena should be considered when Iran winter precipitation variability is studied.

The simultaneous influence of both NIO SSI (W – mode 1) and ENSO on winter precipitation in Iran (A – mode 1) was also investigated by separating precipitation time series into three parts (years with simultaneous occurrence of El Niño and warm NIO SST, La Niña and cold NIO SST, and neutral years). The results of the two-tailed *t*-test (for mean) and Mann–Whitney test (for median) showed that the difference between the mean (and also median) of the El Niño–warm SST years and neutral years is statistically insignificant, but the difference between La Niña–cold SST and neutral years and also El Niño–warm SST is significant at the 5% and 1% level, respectively (Table 5), indicating less influence of El Niño–warm SST on Iran winter precipitation.

Table 4 | Partial correlation and running correlation between Iran winter precipitation (A-mode 1), SOI, and W-mode 1 SST

	Precipitation–SST	**Precipitation–SOI**
Partial correlation	0.15	−0.21
Median running correlation	0.67	−0.56

Table 5 | *P*-value for Mann–Whitney test and *t*-test (number in parentheses) between Iran winter precipitation (A-mode 1), SOI, and W-mode 1 SST

	El Nino–warm SST	**Neutral**	**La Nino–cold SST**
El Nino–warm SST	1	0.27 (0.25)	0.01 (0.01)
Neutral		1	0.05 (0.04)
La Nino–cold SST			1

Values less than 0.01 and 0.05 are significant at 1% and 5% level, respectively.

The investigation of simultaneous occurrence of both events in the highest and lowest 20% of the normalized precipitation (wet and dry years, respectively) suggests that 75% of the winter dry conditions are associated with the concurrent occurrence of positive SOI and negative normalized SST in W – mode 1 region. This value for very dry years (lowest 10%) is 100%. On the other hand, only about 38% of wet years are accompanied by negative SOI and positive normalized SST (50% for very wet years) (not shown), suggesting that simultaneous occurrence of positive SOI and negative normalized SST in W – mode 1 has more effect on Iran winter precipitation variability than the simultaneous occurrence of negative SOI and normalized positive SST.

CONCLUSIONS

This study examined the individual and combined influence of NIO SST and ENSO on winter precipitation variability over Iran during the period 1975–2014. For this purpose, a CCA, running correlation, and partial correlation technique were used. Our results lead to the following conclusions:

- The strongest relationship is found between SST anomaly in the western parts of the NIO (W – mode 1) and Iran winter precipitation (A – mode 1). The relationship is also of warm (cold) – wet (dry) type.

- The influence of the NIO SST on Iran winter precipitation has become weak but statistically significant (in 25-year running correlation) in recent years. In contrast to SST–precipitation relationship, the linkage between precipitation and SOI in recent years is stronger compared to the previous years. It is worth mentioning that the short-term studied period is a constraint in data analysis.
- The correlation of W – mode 1 SST and ENSO index is significant in recent years (since 1993). Since 1993, the ENSO events have been twice that of earlier and most of the El Niño/La Niña events are coincident with positive/negative STT anomaly in NIO.
- The results of the partial correlation analysis suggest that the ENSO index has more influence than NIO SST on Iran winter precipitation.
- It is more likely that, during La Niña and below normal NIO SST, Iran is seriously affected by winter drought, while the wet condition is more likely during the simultaneous occurrence of El Niño and above normal NIO SST.

ACKNOWLEDGEMENTS

This work was supported by Shahrekord University (Grant No. 95GRD1M1605). The author really appreciates it.

REFERENCES

Barnston, A. G. & Tippett, M. K. 2017 Do statistical pattern corrections improve seasonal climate predictions in the North American multimodel ensemble models? *Journal of Climate* **30** (20), 8335–8355.

Berri, G. J. & Bertossa, G. I. 2004 The influence of the tropical and subtropical Atlantic and Pacific Oceans on precipitation variability over Southern Central South America on seasonal time scales. *International Journal of Climatology* **24** (4), 415–435.

Cordery, I. & Opoku-Ankomah, Y. 1994 Temporal variation of relations between sea surface temperature and New South Wales rainfall. *Australian Meteorological Magazine* **43** (2), 73–80.

Diaz, A. F., Studzinski, C. D. & Mechoso, C. R. 1998 Relationships between precipitation anomalies in Uruguay and Southern Brazil and sea surface temperature in the Pacific and Atlantic Oceans. *Journal of Climate* **11** (2), 251–271.

Dong, B. & Dai, A. 2015 The influence of the interdecadal Pacific oscillation on temperature and precipitation over the globe. *Climate Dynamic* **45** (9), 2667–2681.

El-Geziry, T. M. 2013 On the diurnal variations of in-situ sea surface temperature (SST) in Alexandria Eastern Harbour, Egypt. *Journal of Operational Oceanography* **6** (2), 1–8.

Ghasemi, A. R. & Khalili, D. 2008 The association between regional and global atmospheric patterns and the winter precipitation in Iran. *Atmospheric Research* **88** (2), 116–133.

Herr, D. & Galland, G. R. 2009 *The Ocean and Climate Change. Tools and Guidelines for Action*. IUCN, Gland, Switzerland.

Houghton, J. T., Meira Filho, L. G., Callendar, B. A., Harris, N., Kattenberg, A. & Maskell, K. 1996 *Climate Change 1995: The Science of Climate Change: Contribution of Working Group I to the Second Assessment Report of the Intergovernmental Panel on Climate Change*. Cambridge University Press, Cambridge.

Krishnamurthy, V. & Kirtman, B. P. 2003 Variability of the Indian Ocean: relation to monsoon and ENSO. *Quarterly Journal of the Royal Meteorological Society* **129** (590), 1623–1646.

Lu, R. & Lu, S. 2015 Asymmetric relationship between Indian Ocean SST and the Western North Pacific Summer Monsoon. *Journal of Climate* **28** (4), 1383–1395.

Ma, J. & Xie, S. 2013 Regional patterns of sea surface temperature change: a source of uncertainty in future projections of precipitation and atmospheric circulation. *Journal of Climate* **26**, 2482–2501.

Manjunatha, B. R., Krishna, K. M. & Raju, Y. N. 2015 Relationship among sea surface temperature, ENSO and Indian Ocean dipole in the Indian Ocean: a clue to recognizing convective systems. *The Open Oceanography Journal* **8** (1), 20–27.

Nagamani, P. V., Ali, M. M., Goni, G. J., Udaya Bhaskar, T. V. S., McCreary, J. P., Weller, R. A., Rajeevan, M., Gopala Krishna, V. V. & Pezzullo, J. C. 2016 Heat content of the Arabian Sea MiniWarm Pool is increasing. *Atmospheric Science Letter* **17** (1), 39–42.

Nazemosadat, M. J. 1996 *The Impact of Oceanic and Atmospheric Indices on Rainfall Variability*. PhD Thesis, University of New South Wales, Australia.

Nazemosadat, M. J. & Ghasemi, A. R. 2006 The influence of the Indian Ocean Sea Surfer Temperature on the winter precipitation in South-western Iran. In: *8th International Conference on Development of Drylands*. International Dryland Development Commission, Beijing.

Nicholls, N. 1987 The use of canonical correlation to study teleconnections. *Monthly Weather Review* **115**, 393–399.

Pillai, P. A. & Mohankumar, K. 2010 Individual and combined influence of El Niño Southern Oscillation and Indian Ocean Dipole on the tropospheric biennial oscillation. *Quarterly Journal of the Royal Meteorological Society* **699** (136), 297–304.

Rasuly, A. A., Babaeian, I., Ghaemi, H. & Zawar, P. 2012 Time series analysis of the pressure of the synoptic pattern centers affecting on seasonal precipitation of Iran. *Journal of Geography and Regional Development* **10** (27), 18–21.
Risbey, J. S., Pook, M. J., McIntosh, P. C., Wheeler, M. C. & Hendon, H. H. 2009 On the remote drivers of rainfall variability in Australia. *Monthly Weather Review* **137**, 3233–3253.
Roxy, M. K., Ritika, K., Terray, P. & Masson, S. 2014 The curious case of Indian Ocean warming. *Journal of Climate* **27** (22), 8501–8509.
Shenoi, S. S. C., Shankar, D. & Shetye, S. R. 1999 On the sea surface temperature high in the Lakshadweep Sea before the onset of the southwest monsoon. *Journal of Geophysical Research* **104** (C7), 15703–15712.
Slonosky, V. C., Jones, P. D. & Davies, T. D. 2001 Atmospheric circulation and surface temperature in Europe from the 18th century to 1995. *International Journal of Climatology* **21**, 63–75.
Wilks, D. S. 1995 *Statistical Methods in the Atmospheric Sciences: An Introduction*. San Diego Academic Press, San Diego.
Yinyin, D., Tao, G., Huiwang, G., Xiaohong, Y. & Lian, X. 2014 Regional precipitation variability in East Asia related to climate and environmental factors during 1979–2012. *Scientific Reports* **4**, 5693.
Yuan, Y., Zhou, W., Yang, H. & Li, C. 2008 Warming in the northwestern Indian Ocean associated with the El Niño event. *Advances in Atmospheric Sciences* **25** (2), 246–252.

First received 16 November 2018; accepted in revised form 4 August 2019. Available online 26 August 2019